The effect of real-time external resistance optimization on microbial fuel cell performance

Pinto, R. P.; Srinivasan, B.; Guiot, S. R.; Tartakovsky, B.

Publisher's version / Version de l'éditeur:
https://doi.org/10.1016/j.watres.2010.11.033
Water Research, 45, 4, pp. 1571-1578, 2011-01-01

WATER RESEARCH 45 (2011) 1571–1578

Available at www.sciencedirect.com

ScienceDirect

journal homepage: www.elsevier.com/locate/watres

The effect of real-time external resistance optimization on microbial fuel cell performance

R.P. Pinto [a,b], B. Srinivasan [b], S.R. Guiot [a], B. Tartakovsky [a,b,*]

[a] Biotechnology Research Institute, National Research Council, 6100 Royalmount Ave., Montréal, Que., Canada H4P 2R2
[b] Departement de Génie Chimique, École Polytechnique Montréal, C.P.6079 Succ., Centre-Ville Montréal, Que., Canada H3C 3A7

ARTICLE INFO

Article history:
Received 23 July 2010
Received in revised form
21 November 2010
Accepted 22 November 2010
Available online 30 November 2010

Keywords:
Microbial fuel cell
External resistance
Optimal control

ABSTRACT

This work evaluates the impact of the external resistance (electrical load) on the long-term performance of a microbial fuel cell (MFC) and demonstrates the real-time optimization of the external resistance. For this purpose, acetate-fed MFCs were operated at external resistances, which were above, below, or equal to the internal resistance of a corresponding MFC. A perturbation/observation algorithm was used for the real-time optimal selection of the external resistance. MFC operation at the optimal external resistance resulted in increased power output, improved Coulombic efficiency, and low methane production. Furthermore, the efficiency of the perturbation/observation algorithm for maximizing long-term MFC performance was confirmed by operating an MFC fed with synthetic wastewater for over 40 days. In this test an average Coulombic efficiency of 29% was achieved.

1. Introduction

The environmental impact of using fossil fuels to produce energy and their low reserves are leading to a search for renewable energy technologies. Electricity production in Microbial Fuel Cells (MFCs) from a variety of highly diluted organic matter, including wastewater, is one of such technologies (Logan and Regan, 2006; Lovley, 2008). When wastewater is used, MFCs perform waste treatment while recovering energy, thus leading to the possibility of energy-producing wastewater treatment plants.

However, the low power density and the restricted output voltage of MFCs limits their industrial application (Pant et al., 2010). Therefore, intense research is now focused on improving MFC power output through the development of new anode and cathode materials (Kang et al., 2003; Logan et al., 2007; Rismani-Yazdi et al., 2008; ter Heijne et al., 2008), better MFC design (Logan, 2010; Logan et al., 2006; Shimoyama et al., 2008), understanding of electron transfer mechanisms (Debabov, 2008; Reguera et al., 2005; Torres et al., 2010), and optimizing operational conditions (Jadhav and Ghangrekar, 2009). Furthermore, stacks of MFCs are used to increase the operating voltage (Aelterman et al., 2006; Ieropoulos et al., 2008) although challenges such as voltage reversal have been encountered (Oh and Logan, 2007), leading to significant efficiency losses.

One simple alternative that is often overlooked is to enhance MFC's power output by controlling the electrical load (i.e. external resistance) thereby always producing the maximum power output (Woodward et al., 2010). As in any electric power source, maximum power is drawn when the external resistance (R_{ext}) equals the power source's internal resistance (Fuel Cell Handbook, 2005). An incorrect selection of R_{ext}, either larger or smaller than the internal resistance

* *Corresponding author*. Biotechnology Research Institute, National Research Council, 6100 Royalmount Ave., Montréal, Que., Canada H4P 2R2. Tel.: +1 514 496 2664; fax: +1 514 496 6265.
E-mail address: Boris.Tartakovsky@nrc-cnrc.gc.ca (B. Tartakovsky).
0043-1354/$ – see front matter
doi:10.1016/j.watres.2010.11.033

(R_{int}), may lead to large losses in power output. The R_{ext} control is an important requirement for industrial application of MFCs, since their R_{int} might vary with changes in operational parameters such as temperature, pH, influent strength, influent composition, and other factors.

The problem of optimizing the external load for power sources has been addressed before by on-line control, and it is often referred to as Maximum Power Point Tracking (MPPT). Woodward et al. (2010) successfully applied and compared several non-model based real-time MPPT methods for tracking optimal R_{ext} in MFCs fed with acetate. However, only short-term performance of the tracking algorithms was evaluated, with no attempt to study long-term consequences of MFC operation at an optimal R_{ext}. Our recent work using a model-based simulation of microbial populations in an MFC suggests a performance decrease due to changes in microbial populations when there is a significant deviation from the optimal MFC electrical load (Pinto et al., 2010a, 2010b, 2010c). In addition, an application of the MPPT technique in the case of an MFC operated on wastewater, a more complex influent, has not been reported. Therefore, the goals of this paper are (i) to study the long-term effect of R_{ext} on electricity and methane production in an MFC and (ii) to verify the applicability of the MPPT technique for optimizing R_{ext} of an MFC fed with wastewater.

2. Materials and methods

2.1. Analytical methods

Acetate, propionate, and butyrate were analyzed on an Agilent 6890 gas chromatograph (Wilmington, DE, USA) equipped with a flame ionization detector. Method details are provided in Tartakovsky et al. (2008).

Chemical oxygen demand (COD) of synthetic wastewater was estimated according to Standard Methods (APHA, 1995). Both total COD (tCOD) and soluble COD (sCOD) values were analyzed.

Gas production in the MFC anodic chamber was measured on-line using glass U-tube bubble counters interfaced with a data acquisition system. Gas composition was measured using a gas chromatograph (6890 Series, Hewlett Packard, Wilmington, DE) equipped with a 11 m × 3.2 mm 60/80 mesh Chromosorb 102 column (Supelco, Bellefonte, PA, USA) and a thermal conductivity detector. The carrier gas was argon. A detailed description of all analytical methods used in the study can be found in Tartakovsky et al. (2008).

2.2. Inoculum and media composition

Each MFC was inoculated with 5 mL of anaerobic sludge with volatile suspended solids (VSS) content of approximately 40–50 g L^{-1} (Lassonde Inc, Rougemont, QC, Canada) and 20 mL of effluent from an operating MFC.

The stock solution of nutrients was composed of (in g L^{-1}): yeast extract (0.8), NH_4Cl (18.7), KCl (148.1), K_2HPO_4 (64.0), and KH_2PO_4 (40.7). Concentration of acetate in the stock solution was varied in order to obtain the desired organic load by adding sodium acetate (20–80 g L^{-1}). Synthetic wastewater stock solution had a tCOD of 48 g L^{-1} and was composed of (in g L^{-1}): pepticase (15.0), beef extract (15.0), yeast extract (9.0), NH_4HCO_3 (5.1), NaCl (2.8), K_2HPO_4 (0.5), and KH_2PO_4 (0.4).

A stock solution of the trace elements contained (in g L^{-1}): $FeCl_24H_2O$ (2), H_3BO_3 (0.05), $ZnCl_2$ (50), $CuCl_2$ (0.03), $MnCl_24H_2O$ (0.5), $(NH_4)_6Mo_7O_{24}4H_2O$ (0.5), $AlCl_3$ (0.5), $CoCl_26H_2O$ (0.5), $NiCl_2$ (0.5), EDTA (0.5), and concentrated HCl (1 mL). One mL of the trace elements stock solution was added to 1 L of deionized water, which was fed to the MFCs (dilution water). Deionized water was used for solution preparation, and the chemicals and reagents used were of analytical grade. All acetate solutions were sterilized by filtration (0.22 μm filtration unit) and maintained at 4 °C, while and synthetic wastewater solution was frozen and maintained at −6 °C until use.

2.3. MFC design, operation, and characterization

Four single-chamber membraneless air-cathode MFCs were constructed using polycarbonate plates. The anodes were made of 5 mm thick carbon felt measuring 10 cm × 5 cm (SGL Canada, Kitchener, ON, Canada). For MFC-1, MFC-2 and MFC-3 the cathodes were made of a gas diffusion electrode with a Pt load of 0.5 mg cm^{-2} (GDE LT 120 EW, E-TEK Division, PEMEAS Fuel Cell Technologies, Somerset, NJ, USA). The MFC-4 cathode was made using ClFeTMPP (TriPorTech GmbH) on carbon Vulcan XC-72R (Cabot) as a precursor and contained 0.4% Fe with a total catalyst (Fe + C) load of 2 mg cm^{-2} (Birry et al., 2010).The electrodes were separated by a J-cloth with a thickness of about 0.7 mm. An external recirculation loop was installed for improved mixing of the anodic liquid. The anodic chamber temperature was maintained at 25 °C by a PID temperature controller (Model JCR-33A, Shinko Technos Co., Ltd., Osaka, Japan) and a heating plate (120 V-10 W, Volton Manufacturing Ltd, Montreal, Qc, Canada).

The electrical load of each MFC was controlled individually by an external resistor. MFC-1 and MFC-2 had a manually controlled external resistors, while the resistors connected to MFC-3 and MFC-4 were computer controlled digital resistors (Innoray, Montreal, QC, Canada) with a resistor variation range from 2.5 Ω to 1000 Ω.

The MFCs were continuously fed with the stock solutions of carbon source (acetate or synthetic wastewater) and dilution water. The carbon source and dilution streams were combined before entering the anodic chamber. MFC-1, MFC-2, and MFC-3 were operated at several influent concentrations, while maintaining a hydraulic retention time (HRT) of 6 h. MFC-4 was operated at an HRT of 13 h. To account for process variability, each mode of operation was maintained long enough to ensure a steady state performance, which was assessed based on on-line measurements of the output voltage. Table 1 summarizes the operating conditions of each MFC.

Polarization tests (PTs) were periodically performed for each MFC. In each PT R_{ext} was disconnected for 30 min, then open circuit voltage (OCV) was measured. Subsequently, the external resistance was re-connected and progressively decreased from 1000 Ω to 5 Ω every 10 min with voltage measurements at the end of each period. The resulting voltage and current values were used to construct polarization curves, i.e. voltage vs. current plots from where the MFC's total (ohmic

Table 1 – MFCs operating conditions.

MFC	Influent	Organic load (g-COD/L_a/day)	R_{ext} setting
1	Acetate	2.1, 4.3 or 8.5	1000 Ω (above R_{int})
2			5 Ω (below R_{int})
3			Optimal ($R_{ext} \sim R_{int}$)
4	Synthetic wastewater	4 or 6	Optimal ($R_{ext} \sim R_{int}$)

and solution) R_{int} was estimated by the slope of the linear region (Fan et al., 2008). Also, cathode and anode open circuit potentials were measured against an Ag/AgCl reference electrode (222 mV vs. normal hydrogen electrode).

The Coulombic efficiency (*CE*) was estimated as:

$$CE = \frac{I^*_{MFC}\Delta t}{\Delta S n F} \quad (1)$$

where I^*_{MFC} is the average current produced by the MFC during Δt [A]; Δt is the time interval (typically one day) used to calculate average current and substrate consumption [s]; ΔS is the amount of substrate consumed [mol-S]; n is the number of electrons transferred per mol of substrate [mol-e^- mol-S^{-1}]; and *F* is the Faraday constant [A s mol-e^{-1}].

Volumetric power output (P_{out}, mW L_a^{-1}) was calculated using measurements of MFC output voltage, a corresponding value of R_{ext}, and MFC anodic chamber volume (L_a). Maximum volumetric power output (P_{max}) was estimated from the power curves (P_{out} vs current) obtained during the polarization tests. Since R_{ext} in the PTs was changed stepwise, the accuracy of P_{max} estimation was improved by using a linear interpolation of the polarization curve in the region of constant voltage drop,

$U_{MFC} = a_0 + a_1 I_{MFC}$, where U_{MFC} is the MFC output voltage (V), I_{MFC} is the MFC current (A), and a_0, a_1 are the regression coefficients. Based on this interpolation, P_{max} was calculated as described in Logan (2008), p. 47 :

$$P_{max} = \frac{a_0^2}{4 a_1 L_a} \quad (2)$$

Notably, for an MFC with small overpotentials a_0 is close to the OCV estimation and a_1 corresponds to R_{int} (Logan, 2008).

2.4. *Maximum power point tracking (MPPT) algorithm*

The perturbation observation (P/O) method is commonly used in MPPT of solar panels (Hua and Shen, 1998). It was selected for this study because of its robustness, demonstrated in short-term MFC tests (Woodward et al., 2010), and its simplicity. The P/O algorithm applied in this work modified R_{ext} with a predetermined amplitude (ΔR) at each iteration. The direction of resistance change was selected by comparing the value of the power output with that at the previous resistance.

The method can be expressed as follows:

$$R_{ext}(k+2) = R_{ext}(k+1) + \Delta R sign\left(\frac{P_{MFC}(k+1) - P_{MFC}(k)}{R_{ext}(k+1) - R_{ext}(k)}\right) \quad (3)$$

where ΔR is the amplitude of change in R_{ext} [Ω]; P_{MFC} is the MFC power output [W]; and *k* is the iteration number.

Once the algorithm converges to an optimum, the R_{ext} will oscillate around this optimum with a maximum distance of ΔR. Therefore, a smaller ΔR can be used to decrease the distance between R_{ext} and the optimal external resistance, but the time of convergence will increase. A detailed description of this algorithm can be found in Woodward et al. (2010).

3. Results and discussion

3.1. *The impact of external resistance on MFC performance*

The effect of R_{ext} on long-term MFC performance was studied by simultaneously operating acetate-fed MFC-1, 2, and 3 at high, low, and optimal R_{ext} settings, respectively, for 30–35 days (Table 1). The selected R_{ext} values were significantly different (e.g high R_{ext} corresponded to 1000 Ω and low R_{ext} corresponded to 5 Ω, Table 1). This approach reduced the impact of MFC performance variability due to the microbiological nature of the process on the comparison of MFC power outputs and other performance parameters at each mode of operation. Throughout the tests, variations in influent acetate concentration were simultaneously imposed for all MFCs. The profile of acetate influent concentration is shown in Fig. 1a.

Acetate concentration measurements in the effluent streams showed similar substrate removal in all MFCs, as can be seen from the values presented in Fig. 1a. At steady state, the effluent acetate concentration varied from 20 to 160 mg L^{-1}. At the same time, power outputs were quite different. Fig. 1b summarizes power production observed throughout the tests. This figure shows that in all MFCs power output began to increase after approximately 3 days of operation, reaching steady state values after 7–10 days. Power outputs at steady state strongly depended on R_{ext} selection with power outputs around 6, 15, and 58 mW L_a^{-1}, observed for MFC-1 (high R_{ext}), MFC-2 (low R_{ext}), and MFC-3 (optimal R_{ext}), respectively. Notably on day 13 the cathode of MFC-3 was punctured and replaced by a new cathode, made of the same material. Following the replacement, MFC-3 power output approached 135 mW L_a^{-1} for about two days before returning to its previous level. This period was excluded from Fig. 1b. Also, due to technical problems, MFC-2 voltage was not recorded between days 8–12, 14.5 to 16.5, and 28.5 to 30.5.

Fig. 1c presents changes in R_{ext} of MFC-3 imposed by the P/O algorithm over time. At startup, R_{ext} value maintained by the algorithm was above 400 Ω, then after about 5 days of operation R_{ext} sharply decreased to values below 40 Ω. This figure also shows R_{int} values estimated for MFC-3 during polarization tests. As expected, the P/O algorithm provided timely adjustment of R_{ext} to maintain it close to R_{int} values, such that the R_{ext} oscillated around the optimum value equal to MFC-3 internal resistance. The profile of R_{int} change in the MFC-2 test was similar to that observed for MFC-3 rapidly decreasing to 15–30 Ω after first 6 days of MFC operation, while R_{int} of MFC-1 remained at around 200 Ω for most of the test.

While the growth of anodophilic microorganisms during the startup period resulted in relatively slow changes in R_{int}, the variations in operating conditions had an almost immediate impact on R_{int} and therefore on MFC performance. The P/O algorithm's ability to track fast variations of operating conditions (e.g. influent composition) during MFC-3 operation

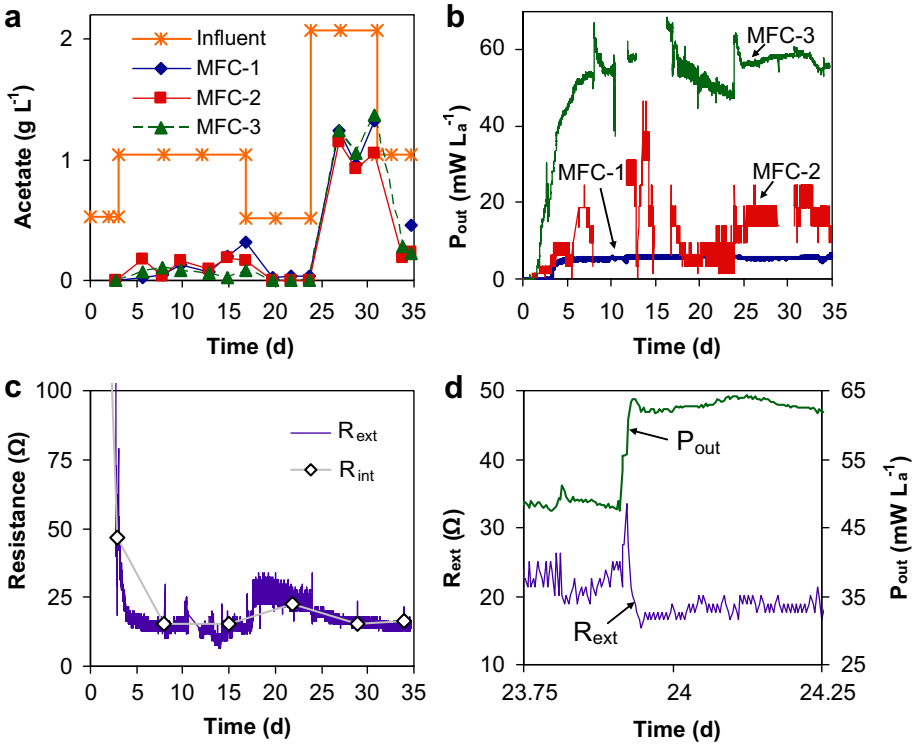

Fig. 1 – (*a*) Acetate concentration in the influent and effluent, and (*b*) power production for MFC-1 MFC-2, and MFC-3 against time; (*c*) R_{ext} and R_{int} values for MFC-3 (MFC-1 and MFC-2 R_{ext} values were always kept at 1000 Ω and at 5 Ω, respectively); (*d*) R_{ext} and P_{out} values during an increase in the MFC-3 influent concentration at t = 23.9 days.

is illustrated in Fig. 1d. Here, the influent acetate concentration was increased from 0.5 to 2 g L^{-1} on day 24. This increase in acetate concentration caused a decrease of R_{int} and, accordingly, the MPPT algorithm decreased the R_{ext} value thus maximizing power output under new operating conditions.

Fig. 2 presents estimations of current density and Coulombic efficiency (*CE*) for MFC-1, MFC-2 and MFC-3. As expected, MFC-1, which was operated at a high R_{ext}, always had a low current density and a low *CE*, while MFC-2 and MFC-3 showed larger values. MFC-2, which was operated at the lowest R_{ext}, was expected to have the highest Coulombic efficiency. However, current densities (Fig. 2a) and *CE* (Fig. 2b) of MFC-3, which was operated at an optimal R_{ext}, on average were slightly higher than that of MFC-2. *CE* calculations showed a more pronounced difference between MFC-2 and MFC-3, however this difference could be attributed to the variability of the effluent acetate measurements. Also, MFC-3 featured the shortest startup time, as can be seen from the comparison of current densities in Fig. 2a.

Polarization tests provided additional information for the comparison of MFC performances. Fig. 3a shows the evolution of the cathode and anode open circuit potentials (OCP) over time. As expected, cathode OCP values were similar for all MFCs and remained constant throughout the experiment. Following the startup, anode OCP values decreased for all MFCs, with the fastest decrease observed for MFC-2 (low R_{ext}),

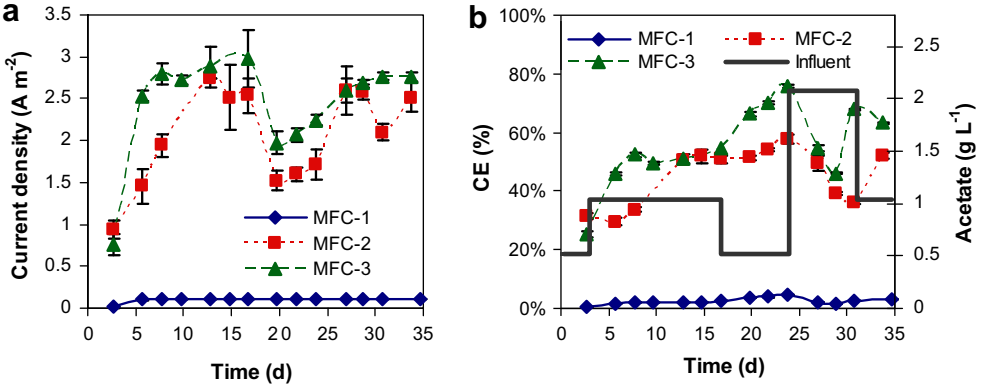

Fig. 2 – Current density (*a*) and Coulombic efficiency (*b*) observed at various acetate loads (Fig. 1a).

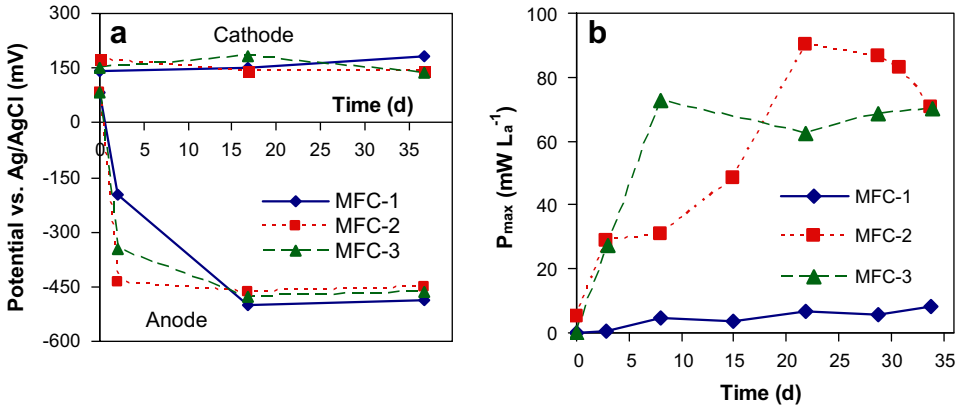

Fig. 3 – (*a*) The evolution of the cathode and anode OCP values over time, and (*b*) maximum power densities estimated using polarization curves according to Eq. (2).

followed by MFC-3 (optimal R_{ext}). MFC-1, which was operated at a high R_{ext}, was the last to reach a steady state value of the anode potential. Nevertheless, the anode OCP values for all MFCs were similar after 15 days of testing. It can be hypothesized that this pattern of anode OCP decrease over time was reflective of anode colonization by the anodophilic microorganisms. Indeed, lower values of R_{ext} facilitate the electron transfer process thus providing growth advantages to the anodophilic microorganisms. Consequently MFC-2 operated at the lowest R_{ext} featured the fastest rate of the anodophilic biofilm formation. However, MFC operation at an R_{ext} below R_{int} results in low power output (Logan, 2008), thus requiring R_{ext} optimization.

When maximal power outputs were estimated from the polarization test results, it was observed that MFC-1 always had low P_{max}, never exceeding 9 mW L_a^{-1}. Maximal power outputs estimated for MFC-2 and MFC-3 increased during the first 15–20 days of the experiment (Fig. 3b). A maximal power output of 95 mW L_a^{-1} was estimated based on the polarization test for MFC-3 on day 15, which was carried out shortly after the cathode replacement in this MFC. As mentioned above, the cathode replacement resulted in higher than usual power output between days 13 and 15. On average, MFC-3 maximal power output remained around 70 mW L_a^{-1}, which agreed well with the power densities measured during MFC-3 test (Fig. 1b). At the same time, power output of MFC-2 during normal operation was very low because of the R_{ext} choice. The selection of R_{ext} for MFC-1 ($R_{ext} = 1000\ \Omega$) and MFC-2 ($R_{ext} = 5\ \Omega$) was confirmed by the polarization tests. After the startup period, R_{int} in MFC-1 varied between 50 and 200 Ω, while in MFC-2 R_{int} varied between 15 and 25 Ω. Thus, MFC-1 was operated at $R_{ext} >> R_{int}$, and MFC-2 was operated at $R_{ext} << R_{int}$ throughout the test, as intended.

Besides power output comparison, methane production in the anodic compartment of each MFC was measured throughout the tests and was used to compare the long-term effects of R_{ext} selection on methane production. Since the MFCs were inoculated with anaerobic sludge, methane production was observed at the beginning of the operation in all MFCs. The methane production in MFC-1 increased over time, while it decreased in MFC-2 and MFC-3. To compare electricity and methane production for MFC-1, MFC-2, and MFC-3 steady state values were calculated using experimental results obtained between day 7 and 30 of MFC operation, when constant organic load was applied. The average methane production rates were 2.0 ± 0.7, 0.2 ± 0.1, 0.6 ± 0.2 mL d^{-1} in MFC-1, MFC-2, and MFC-3, respectively. The corresponding power outputs for these MFCs were 5.6 ± 0.3, 14.6 ± 7.7, and 60.8 ± 17.2 mW L_a^{-1}. It should be acknowledged that methane flow measurements were complicated by the small volume (50 mL) of the anodic compartments and low methane production rates, in the range of several mL per day. Measurements of such small flow rates resulted in large standard deviations. Nevertheless, the overall trends were clear showing significantly higher methane production in MFC-1 operated at high R_{ext}. In contrast, methane production in MFC-1 and MFC-2 was very low. These results agree with methane production measurements reported in Martin et al. (2010), where MFCs were operated at R_{ext} above estimated values of R_{int} resulting in significant methane production. It was previously demonstrated using biomolecular methods, that a high R_{ext}, which implies MFC operation at more positive anode potentials, decreases the amount of the anodophilic microorganisms (Torres et al., 2009).

There is a significant body of evidence proving that the external resistance at which the MFC operates has an influence on the microbial communities and the long-term performance (Aelterman et al., 2008; Chae et al., 2010; Lyon et al., 2010; Pinto et al., 2010c; Torres et al., 2009). Aelterman et al. (2008) observed the impact of R_{ext} on electricity and methane production in an MFC inoculated with a mixed anaerobic culture and concluded that low methane production and stable power output are only obtained if R_{ext} is set close to the MFC internal resistance. Furthermore, Chae et al. (2010) compared methanogenic activity and methane production in MFCs subjected to several external perturbations (pH, temperature, oxygen exposure, addition of a methanogenesis inhibitor, and R_{ext} variation). They also concluded that electricity production was increased and methane production was decreased only when a methanogenesis inhibitor (BES, 2-bromoethanesulfonate) was added to the anodic chamber or by setting a R_{ext} close to the R_{int} values.

Computer simulations using a two population MFC model (Pinto et al., 2010c) corroborated with the experimental

evidence above. The model was used to simulate the outcome of the competition between the anodophilic and methanogenic microorganisms for a common carbon source (acetate) in MFCs operated at different organic loads and R_{ext} settings (Pinto et al., 2010c). It was predicted that, independent of the microbial composition of the inoculum, proliferation of the anodophilic microorganisms could only be achieved at R_{ext} values that are equal to or less than the MFC internal resistance. The same conclusion can be inferred from the results of Lyon et al. (2010). In this study the microbial composition of biofilms sampled from MFCs inoculated with the same sludge and operated at different R_{ext} values were analyzed. By using Ribosomal Intergenic Spacer Analysis (RISA) they demonstrated, based on the profiles observed, that the microbial community structure in MFC's biofilm operated at R_{ext} appreciably above R_{int} (1 kΩ and 10 kΩ) was significantly different from that observed in the MFC operated at low R_{ext} (10 Ω, 100 Ω, and 470 Ω). As mentioned above, a low R_{ext} promotes growth and metabolic activity of the anodophilic microorganisms since electron transport to the cathode is facilitated. However R_{ext}, which is lower than the MFC R_{int} value leads to a low power output, i.e. an optimal R_{ext} value ($R_{ext} \sim R_{int}$) should be maintained. Notably, all of the tests mentioned above were carried out by manual adjustment of R_{ext} without using a real-time algorithm, which would guarantee timely correction of R_{ext}.

The results from the citations above are in perfect agreement with the findings presented in this paper, where acetate-fed MFCs were inoculated with the same anaerobic sludge and consumed comparable quantities of carbon source. They were operated at high, low, or optimal R_{ext} settings, leading to Coulombic efficiencies remarkably different (Fig. 2b). High R_{ext} led to, essentially, an anaerobic reactor with low Coulombic efficiency and significant methane production. At the same time, both MFC-2 (low R_{ext}) and MFC-3 (optimal R_{ext}) featured high Coulombic efficiency, and by the end of the 30 day test methane production in these MFCs declined to near zero values. Notably, the high power output with negligible methane production observed during MFC-3 operation are in agreement with the results of ClFeTMPP cathode tests, where an MFC was also operated using the P/O algorithm for the on-line optimization of R_{ext} (Birry et al., 2010). Considering that MFC operation at R_{ext} values below R_{int} leads to a sharp drop in power output (Fuel Cell Handbook, 2005), it is sufficient to maintain R_{ext} at an optimal value in order to minimize methane production and maximize power production.

3.2. *MFC operation on synthetic wastewater*

The efficiency of the P/O algorithm when operating an MFC on a complex feed was confirmed by feeding MFC-4 with synthetic wastewater. The power output observed during this test and R_{ext} values selected by the P/O algorithm are shown in Fig. 4. This graph also shows R_{int} estimations obtained in the polarization tests. A sharp decrease in R_{int} values obtained from the polarization tests and R_{ext} values selected by the P/O algorithm can be seen after the first 5 days of MFC operation (Fig. 4c). After this point, R_{int} remained between 20 Ω and 60 Ω with R_{ext} matching these values. As one can see, P_{out} increased steadily during the first 15 days of the experiment (Fig. 4b), which is longer than the 5 day startup period observed in the acetate-fed MFC-3 (Fig. 1b). A longer startup period could be attributed to the use of synthetic wastewater containing complex organic matter. We hypothesize that wastewater hydrolysis and fermentation steps, which were required because of the complex wastewater composition, limited the amount of volatile fatty acids available for growth and metabolism of the anodophilic microorganisms.

To demonstrate the robustness of the P/O algorithm, MFC-4 was subjected to two types of perturbations: First the organic load was increased by 50% between days 16 and 20 (Fig. 4a), then between days 23 and 33 the MFC temperature was increased from 25 °C to 35 °C (Fig. 4d). The increase in organic load did not result in a substantial increase of power production and R_{int} remained unchanged (Fig. 4b,c). It can be seen that the increased organic load did not result in an immediate increase in the effluent COD concentration (Fig. 4a), likely due to a short duration of the test. Effluent VFA analysis showed that concentrations of acetate, propionate, and butyrate always remained below 70–90 mg L^{-1} during the test. Apparently, the biotransformation process was limited by the rate of hydrolysis rather than the rate of VFA consumption by the anodophilic microorganisms. Accordingly, R_{int} remained unchanged during the test. MFC response to temperature increase was more pronounced with an immediate drop in R_{ext} from about 48 Ω to 30 Ω (40% decrease) and a 50% increase of P_{out}. Once MFC temperature was returned to 25 °C, the P/O algorithm adjusted R_{ext} close to its previous level. A similar response to a temperature perturbation was observed by Woodward et al. (2010).

Notably, an additional external perturbation during MFC-4 test was caused by the fermentation of the synthetic wastewater solution kept at room temperature in a syringe. This feeding solution was replaced every two or three days. Fermentation of the synthetic wastewater resulted in a visible change in the feed solution appearance with an average of 0.15 g L^{-1} of volatile fatty acids at the end of each feeding period, although tCOD concentration remained constant. The arrows in Fig. 4b represent the times when the synthetic wastewater was replenished. It can be seen that synthetic wastewater fermentation had a direct impact on the P_{out}. After each wastewater replenishment the MFC power output declined for about 24 h, while reaching its maximal values by the end of each feeding period. Also, abrupt drops in P_{out} observed on days 25, 28, and 33 are related to delays in replacing the syringe, which resulted in an interruption of the feed. These perturbations of the organic load were promptly followed by the P/O algorithm thus demonstrating its excellent robustness, as can be seen from the results presented in Fig. 4b.

Polarization tests not only confirmed the choice of R_{ext} values by the P/O algorithm, but also demonstrated time-related changes in OCV and P_{max} values resulting from MFC operation at an optimal R_{ext}. OCV and P_{max} values presented in Fig. 5 show that OCV slowly increased in about 20 days stabilizing around 500 mV, while P_{max} more then doubled after day 7 and fluctuated between 17 and 35 mW L_a^{-1} with higher outputs observed by the end of the test. Overall, the Coulombic efficiency of MFC-4 varied between 14% and 41%, with an average of 29% throughout the experiment.

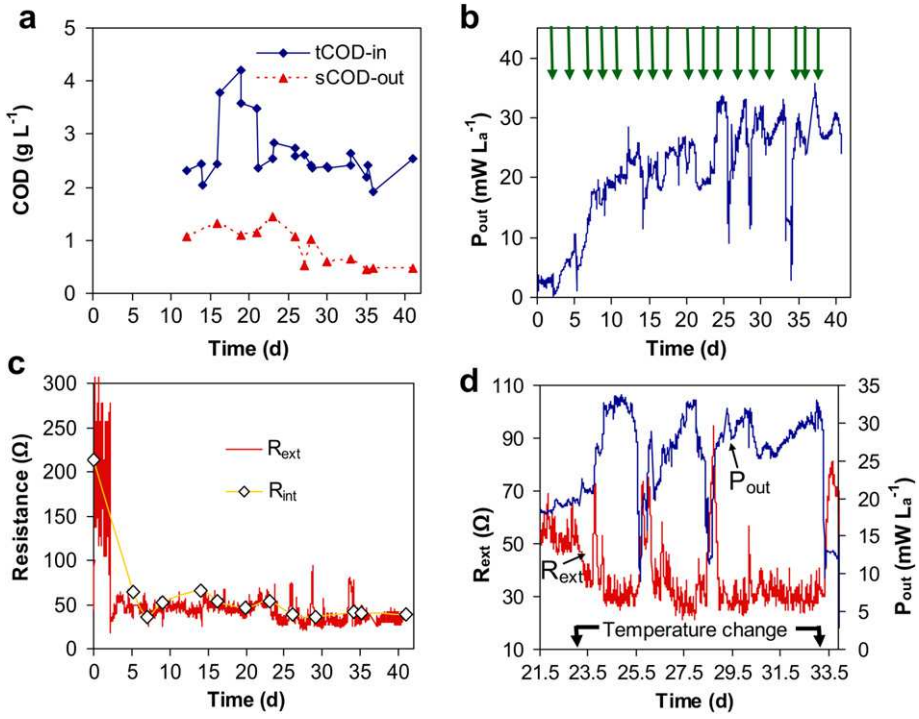

Fig. 4 – MFC-4 performance: (*a*) total COD in the influent (tCOD-in) and soluble COD in the effluent (sCOD-out). The organic load was increased by 50% between days 16 and 20; (*b*) power output; (*c*) external and internal resistance; (*d*) External resistance and power density response during an increase in temperature from 25 °C to 35 °C at 23.25 days. Arrows show syringe replacement times.

During MFC-3 and MFC-4 operation, real-time correction of R_{ext} was instrumental in maintaining its value at or close to R_{int}. Indeed, because of the variations of organic load, composition, and MFC temperature during the tests, the internal resistance of the MFCs varied in time. Polarization tests performed after each change in operating conditions were used to estimate R_{int} variations, as can be seen in Fig. 1c and Fig. 4c, where R_{int} estimations are shown along with R_{ext} values selected by the P/O algorithm. The P/O algorithm demonstrated excellent stability and fast convergence so that

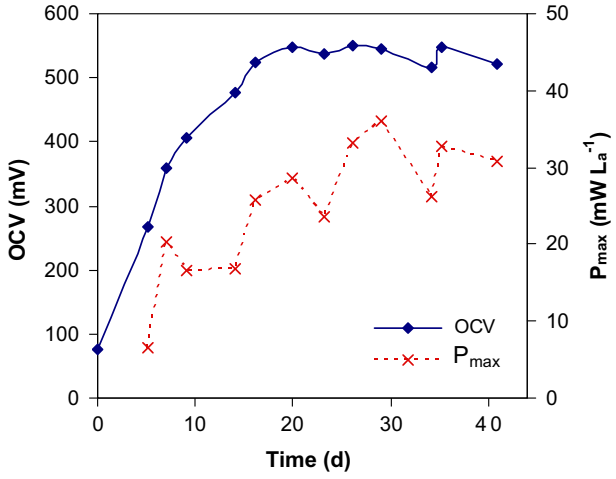

Fig. 5 – Open circuit voltage and maximum power output estimated from the polarization tests in MFC-4.

R_{ext} always remained close R_{int} as illustrated in Fig. 1d and Fig. 4d. The real-time strategy for R_{ext} control also allowed for avoiding a sharp decrease in MFC performance even when MFC feed was interrupted due to a technical problem (e.g. syringe pump malfunction or a delay in syringe replacement). These events led to a sharp short-term increase in the internal resistance, which was successfully tracked by the P/O algorithm (e.g. days 25, 28 and 33 in Fig. 4c). Notably, implementing an MPPT on-line technique for MFC's R_{ext} control could be used for individual control of electric loads of MFC stacks. This strategy might prevent MFC operation at R_{ext} values below its R_{int} thus helping to avoid voltage reversal (Oh and Logan, 2007) after a feed disruption or another operating problem.

4. Conclusion

In this study, a simple perturbation/observation algorithm was used to maximize MFC power output by matching R_{ext} and R_{int} values. The real-time optimization of R_{ext} was tested through long-term operation of MFCs fed with either acetate or synthetic wastewater. The P/O algorithm demonstrated an excellent performance when the MFC was subject to perturbations in operating conditions such as variations in organic load, influent composition, and temperature. A comparison of MFC performance at an optimal R_{ext} value, with MFCs operated at either high ($R_{ext} >> R_{int}$) or low ($R_{ext} << R_{int}$) external resistances showed that real-time resistance optimization led to significantly higher power outputs with less methane

production. MFCs operated at an optimal resistance showed average Coulombic efficiencies of 57% and 29% on acetate and synthetic wastewater, respectively. It is concluded that the real-time optimal control of MFC electrical load might be instrumental in the development of stackable MFCs for combined wastewater treatment and power production.

Acknowledgement

This research was supported by the National Research Council of Canada (NRC publication #53342).

REFERENCES

Aelterman, P., Rabaey, K., Pham, H.T., Boon, N., Verstraete, W., 2006. Continuous electricity generation at high voltages and currents using stacked microbial fuel cells. Environmental Science and Technology 40 (10), 3388–3394.

Aelterman, P., Versichele, M., Marzorati, M., Boon, N., Verstraete, W., 2008. Loading rate and external resistance control the electricity generation of microbial fuel cells with different three-dimensional anodes. Bioresource Technology 99 (18), 8895–8902.

APHA, 1995. Standard Methods for the Examination of Water and Wastewater. American Public Health Association, Washington, DC.

Birry, L., Mehta, P., Jaouen, F., Dodelet, J.P., Guiot, S.R., Tartakovsky, B., 2010. Application of iron-based cathode catalysts in a microbial fuel cell. Electrochimica Acta, in press.

Chae, K.-J., Choi, M.-J., Kim, K.-Y., Ajayi, F.F., Park, W., Kim, C.-W., Kim, I.S., 2010. Methanogenesis control by employing various environmental stress conditions in two-chambered microbial fuel cells. Bioresource Technology 101 (14), 5350–5357.

Debabov, V., 2008. Electricity from microorganisms. Microbiology 77 (2), 123–131.

Fan, Y., Sharbrough, E., Liu, H., 2008. Quantification of the internal resistance distribution of microbial fuel cells. Environmental Science and Technology 42, 8101–8107.

Fuel Cell Handbook, 2005. National Energy Technology Laboratory U.S. Department of Energy. University Press of the Pacific.

Hua, C., Shen, C., 1998. Comparative Study of Peak Power Tracking Techniques for Solar Storage System. In: Anon (Ed.). IEEE, Anaheim, CA, USA, pp. 679–685.

Ieropoulos, I., Greenman, J., Melhuish, C., 2008. Microbial fuel cells based on carbon veil electrodes: stack configuration and scalability. International Journal of Energy Research 32, 1228–1240.

Jadhav, G.S., Ghangrekar, M.M., 2009. Performance of microbial fuel cell subjected to variation in pH, temperature, external load and substrate concentration. Bioresource Technology 100 (2), 717–723.

Kang, K.H., Jang, J.K., Pham, T.H., Moon, H., Chang, I.S., Kim, B.H., 2003. A microbial fuel cell with improved cathode reaction as a low biochemical oxygen demand sensor. Biotechnology Letters 25 (16), 1357–1361.

Logan, B., Cheng, S., Watson, V., Estadt, G., 2007. Graphite fiber brush anodes for increased power production in air-cathode microbial fuel cells. Environmental Science and Technology 41, 3341–3346.

Logan, B.E., 2008. Microbial Fuel Cells. John Wiley & Sons, Hobeken, New Jersey.

Logan, B.E., 2010. Scaling up microbial fuel cells and other bioelectrochemical systems. Applied Microbiology and Biotechnology 85 (6), 1665–1671.

Logan, B.E., Hamelers, B., Rozendal, R.A., Schroder, U., Keller, J., Freguia, S., Aelterman, P., Verstraete, W., Rabaey, K., 2006. Microbial fuel cells: methodology and Technology. Environmental Science and Technology 40 (17), 5181–5192.

Logan, B.E., Regan, J.M., 2006. Microbial fuel cells - Challenges and applications. Environmental Science and Technology 40 (17), 5172–5180.

Lovley, D.R., 2008. The microbe electric: conversion of organic matter to electricity. Current Opinion in Biotechnology 19 (6), 564–571.

Lyon, D.Y., Buret, F., Vogel, T.M., Monier, J.-M., 2010. Is resistance futile? Changing external resistance does not improve microbial fuel cell performance. Bioelectrochemistry 78 (1), 2–7.

Martin, E., Savadogo, O., Guiot, S.R., Tartakovsky, B., 2010. The influence of operational conditions on the performance of a microbial fuel cell seeded with mesophilic anaerobic sludge. Biochemical Engineering Journal 51 (3), 132–139.

Oh, S.E., Logan, B.E., 2007. Voltage reversal during microbial fuel cell stack operation. Journal of Power Sources 167 (1), 11–17.

Pant, D., Van Bogaert, G., Diels, L., Vanbroekhoven, K., 2010. A review of the substrates used in microbial fuel cells (MFCs) for sustainable energy production. Bioresource Technology 101 (6), 1533–1543.

Pinto, R.P., Perrier, M., Tartakovsky, B. and Srinivasan, B., 2010a. Performance analyses of microbial fuel cells operated in series, Proceedings of 9th International Symposium on Dynamics and control of process systems, Leuven, Belgium.

Pinto, R.P., Srinivasan, B., Manuel, M.F., Tartakovsky, B., 2010b. A two-population bio-electrochemical model of a microbial fuel cell. Bioresource Technology 101 (14), 5256–5265.

Pinto, R.P., Tartakovsky, B., Perrier, M., Srinivasan, B., 2010c. Optimizing treatment performance of microbial fuel cells by reactor Staging. Industrial & Engineering Chemistry Research 49 (19), 9222–9229.

Reguera, G., McCarthy, K.D., Mehta, T., Nicoll, J.S., Tuominen, M.T., Lovley, D.R., 2005. Extracellular electron transfer via microbial nanowires. Nature Biotechnology 435, 1098–1101.

Rismani-Yazdi, H., Carver, S.M., Christy, A.D., Tuovinen, I.H., 2008. Cathodic limitations in microbial fuel cells: an overview. Journal of Power Sources 180, 683–694.

Shimoyama, T., Komukai, S., Yamazawa, A., Ueno, Y., Logan, B.E., Watanabe, K., 2008. Electricity generation from model organic wastewater in a cassette-electrode microbial fuel cell. Applied Microbiology and Biotechnology 80 (2), 325–330.

Tartakovsky, B., Manuel, M.F., Neburchilov, V., Wang, H., Guiot, S.R., 2008. Biocatalyzed hydrogen production in a continuous flow microbial fuel cell with a gas phase cathode. Journal of Power Sources 182 (1), 291–297.

ter Heijne, A., Hamelers, H.V.M., Saakes, M., Buisman, C.J.N., 2008. Performance of non-porous graphite and titanium-based anodes in microbial fuel cells. Electrochemica Acta 53, 5697–5703.

Torres, C.I., Krajmalnik-Brown, R., Parameswaran, P., Marcus, A.K., Wanger, G., Gorby, Y.A., Rittmann, B.E., 2009. Selecting anode-respiring bacteria based on anode potential: phylogenetic, electrochemical, and microscopic characterization. Environmental Science and Technology 43 (24), 9519–9524.

Torres, C.I., Marcus, A.K., Lee, H., Parameswaran, P., Krajmalnik-Brown, R., Rittmann, B.E., 2010. A kinetic perspective on extracellular electron transfer by anode-respiring bacteria. FEMS Microbiology Reviews 34 (1), 3–17.

Woodward, L., Perrier, M., Srinivasan, B., Pinto, R.P., Tartakovsky, B., 2010. Comparison of real-time methods for maximizing power output in microbial fuel cells. AIChE Journal 56 (10), 2742–2750.